ROSE 2007 - IEEE International Workshop
on Robotic and Sensors Environments
Ottawa - Canada, 12-13 October 2007

Autonomous Stair Climbing with Reconfigurable Tracked Mobile Robot

Pinhas Ben-Tzvi, Shingo Ito, and Andrew A. Goldenberg
Robotics and Automation Laboratory
Department of Mechanical and Industrial Engineering, University of Toronto
5 King's College Rd., Toronto, ON, Canada M5S 3G8
{bentzvi, ito, golden}@mie.utoronto.ca

***Abstract*— Mobile robots have been developed for surveillance, reconnaissance and inspection as well as for operation in hazardous environments. Some are intended to explore not only natural terrains but also artificial environments, including stairs. This paper explores algorithms to autonomously climb stairs. The algorithms were derived and implemented for a specific mobile robot with the ability to traverse such obstacles by changing its tracks configuration. Furthermore, algorithms have been developed for conditions under which the mobile robot halts its motion during the climbing process when at risk of flipping over or falling down. The technical problems related to the implementation of some of these functions have been identified and analyzed, and their solutions validated and tested. The algorithms and solutions were validated experimentally, illustrating the effectiveness of autonomous climbing of stairs.**

***Keywords*—mobile robot, autonomous climbing, control architecture, robot sensors.**

I. Introduction

Mobile robots have been developed for surveillance, reconnaissance and inspection. Some are intended to explore not only natural terrains, but also artificial environments, including stairs and ramps. Traversing such urban obstacles has been an inevitable difficulty to the improvement of mobility and expansion of surveillance ranges. In this paper we present development and implementation of algorithms and their application for autonomous climbing of stairs with a Linkage Mechanism Actuator (LMA) tracked mobile robot developed with Engineering Services Inc. (ESI) [1].

Before the implementation of autonomous climbing, LMA had two modes of operation. In the manual mode, an operator drives LMA directly with the use of the remote controller. In the pre-programmed mode, a trajectory can be inputted beforehand, and LMA will follow the path automatically. During operations and demonstrations of stair climbing, the manual mode was utilized, and the operator navigated LMA using the remote controller with a joystick and control panel. The disadvantage of this mode is that the operator had to rely on his/her own judgment to set the robot in the right configuration to be able to successfully climb stairs.

First, the operation of the manual mode is intuitive, and it would be almost impossible to exactly rotate wheels or joints to certain angles. This is because the motions are always confirmed by the operator watching LMA. Thus, the operation of LMA depends on the operator's emotional and physical conditions, and they are not always ideal.

Second, climbing stairs in the manual mode requires the operator's knowledge, experiences, skills and training. The procedures of climbing stairs are composed of several motions, which operators must know thoroughly. This is not preferable since operators generally prefer less information to use a product. Training on ascending stairs is also not preferable, as practices usually include failures. In the worst case, LMA might fall off the stairs, resulting in a critical damage to the system.

Finally, the manual mode is unsuitable for teleoperated climbing over a blindfold such as a wall, fence or hedge. An operator must watch LMA while climbing stairs to confirm the robot's motions. Once LMA disappears from the visual field, it would be out of control. Even if it might be possible to observe the location of LMA and its configuration with the aid of the equipped Pan Tilt Zoom camera (PTZ), climbing stairs over a blindfold would demand enormous time, effort and skill.

To solve the problems listed above; autonomous climbing of stairs was researched and successfully implemented.

II. Mechanical Architecture of the Mobile Robot and Embedded Sensors

A. Mechanical Structure of LMA

Several mechanisms of robots to ascend stairs are currently available. Traversing stairs by connecting small identical robots is one approach [2],[3]. One unique strategy is a single miniature robot that jumps to traverse each step [4]. More commonly, robots with legs or leg and wheel combinations are used [5],[6]. Tracked robots with special linkages are also widely used. Some robots such as the ROBHAZ-DT3 have uncontrollable linkages [18]. On the other hand, other robots such as PackBot, Urban and Andros Mark VI have an actuated linkage for additional tracks [8]-[10]. LMA also has an actuated linkage, but this is for reconfigurable tracks, not additional ones.

Several views of LMA are shown in Fig. 1. The mobile robot has two fixed wheels at the front and rear of the chassis. Two arms are installed on both flanks of the frame, and two wheels are attached at their tip via a spring loaded prismatic joint to retain tension in each track. The arms are rotated together in parallel to each other by one motor. The set of the two arms, including the attached joints and wheels mounted on them, is called “flipper”. By rotating the flipper, the track configuration changes, which facilitates getting over obstacles, climbing and descending stairs and slopes. Each track is rotated by a motor independently, so that LMA can not only go forward and backward, but also turn left, right and around. An anchor is also available on the frame to install an optional robotic arm.

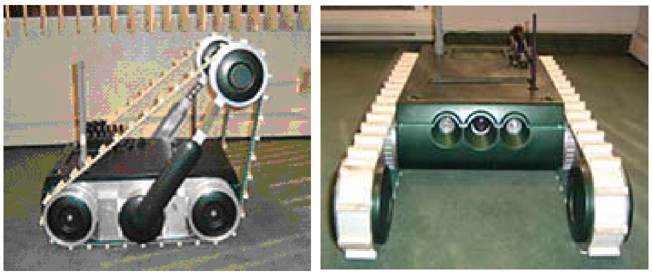

(a) Side view (b) Front view

Fig. 1 Side and front views of the LMA

Relationship of Flipper Angle and Length

The tracks are flexible enough to allow the flipper rotation, but their length never changes. Therefore, the trajectory of the flipper tip follows an ellipsoid trajectory, and the relationship of a flipper angle and its corresponding flipper length was calculated and is given by equation (1). The parameters used for the calculation are defined in Fig. 2. The flipper angle is denoted by φ, and its value is zero degrees when the flipper is extended to the front. The flipper length is denoted by $l(\varphi)$, which is the distance between the flipper tip and the flipper joint located at the center of the chassis. The longest and shortest lengths the flipper can provide are denoted by *a* and *b,* respectively. The shortest flipper length is achieved by setting the flipper perpendicular to the frame (i.e., $\varphi = \pm 90^o$), while the longest flipper length is achieved when the flipper extends to the front or rear (i.e., $\varphi = 0^o$ or $\varphi = 180^o$).

$$l(\varphi) = \sqrt{\frac{a^2 b^2}{b^2 \cos^2 \varphi + a^2 \sin^2 \varphi}} \qquad (1)$$

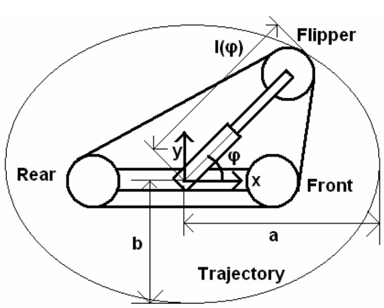

Fig. 2 Parameters for flipper length calculation

Some specifications of the LMA are provided in Table 1.

Table 1 General specification of the LMA

Name	Parameter	Dimension
Wheelbase	L	400 mm
Longest Flipper Length	a	466 mm
Shortest Flipper Length	b	421 mm
Wheel Radius	r	74 mm
Weight	w	34.0 kg

Of the three motors situated in the robot chassis, two motors are propelling the left and right tracks and the third one is propelling the flipper. Encoders connected to the motors are utilized to establish closed-loop position, speed or acceleration control of the motors.

Sensors

The LMA is equipped with a thermometer, GPS, three-axis compass and battery-voltage monitor. The three-axis compass manufactured by Honeywell provides pitch, roll and yaw (heading direction) angle with a sampling frequency of 8Hz. The range of the heading direction is 360^0 and that of roll and pitch angles is $\pm 60^0$. The package is composed of single and two-axis magnetic sensors, as well as a two-axis accelerometer.

B. Stair Climbing Procedure

The schematic in Fig. 3 shows the stair profile used and some relevant parameters. The height of each step or riser length ranges from 12 to 18 cm and the width of a step ranges from 8 to 25 cm. The imaginary line connecting the stair edges is referred to as the nose line. The slope of a nose line indicates how steep the stairs are, and its range is from 25 to 45^0. Stairs with step height and width of 18 cm and nose line slope of 45^0 were used to test LMA.

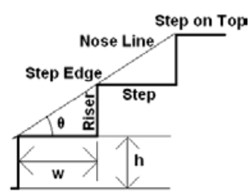

Fig. 3 Stair profile and parameters

The motions required to climb stairs are broken down into three stages: “riding on nose line”, “going on nose line” and “landing”. Fig. 4 shows the complete procedure to climb stairs [2]. In the riding on nose line stage, LMA moves forward until its front wheels are above the first step edge as shown in Fig. 4(a), (b) and (c). During the motion, the flipper is set at a certain angle (approx. 45^0) at the front, such that some of the treads on the tracks hook onto the first step edge. Then, the flipper is rotated backwards at least until its tip touches the ground to avoid flipping over as the climbing starts (Fig. 4(d)) and LMA moves forward (Fig. 4(e)). At a proper time, LMA is stopped and the flipper is fully extended to the rear to ride on the nose line as shown in Fig. 4(f).

After the completion of the riding on nose line stage, LMA moves forward on the nose line (going on nose line stage).

LMA maintains this stage until the front wheels are suspended above the step at the top. During this stage, the operator would be required to adjust the heading direction of LMA, for example, in cases of curved stairs or spiral stairs.

The purpose of the landing stage is to prevent from the front wheels to hit the step at the top. In order to do so, the flipper is slightly rotated downwards as shown in Fig. 4(g). Subsequently, LMA moves forward until its rear wheels are completely placed on the step at the top, and its flipper fully extended to the rear (Fig. 4(h)). In cases where "hard landing" is acceptable, it may not be required for operators to follow the landing procedure and it can be skipped during the autonomous climbing procedure.

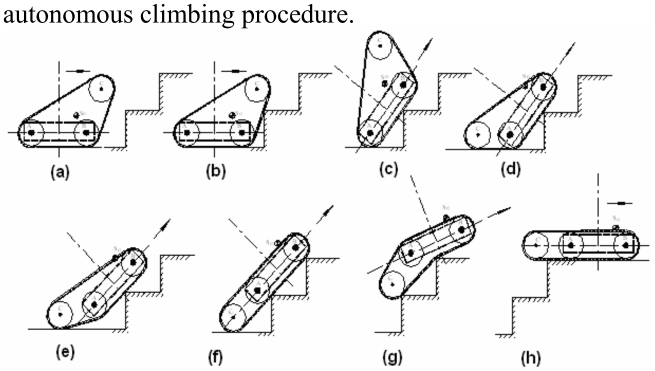

Fig. 4 Climbing procedure for stairs
Climbing follows the order of (a), (b), (c), (d), (e), (f), (g) and (h)

III. Stability Analysis Algorithm for Climbing Stairs

During autonomous climbing of stairs, there was a considerable probability that LMA would fall off or flip over. To address such scenarios and relate them to the configuration and inclination of the robot, stability judgment equations were formulated. By calculating the inclination thresholds that result in unstable positions and by adding certain margins to them, LMA was successfully stopped before it was in danger of tipping or falling off. Here, the required equations and algorithms for some cases are derived and introduced.

A. Stability Judgment Equations

To stop LMA or to avoid unstable positions, the inclination thresholds related to LMA stability were derived for the configurations used in autonomous climbing. The derived equations are called stability judgment equations. The mathematical relationship between the flipper angle φ .and LMA inclination θ is also derived with respect to specific configurations as follows: (i) stability judgment equation of LMA with flipper suspended; (ii) with flipper at the rear; and (iii) LMA on nose line.

(i) Stability Judgment Equation of LMA – Flipper Suspended

The configuration to be considered is depicted in Fig. 5(a), showing the front wheels on the first step edge and the flipper suspended in the air. A Cartesian coordinate frame is aligned with the origin located at the center of the rear wheels and its x axis is parallel with the robot's frame. On this coordinate frame, the location of center of gravity of LMA is expressed as G_x and G_y with respect to x and y axis, respectively.

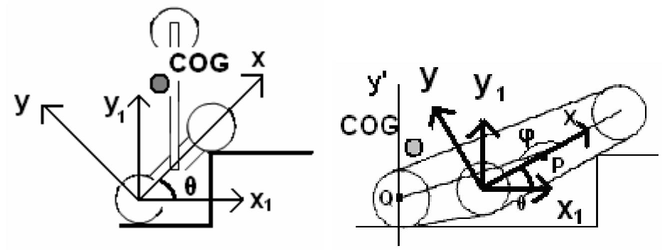

(a) (b)

Fig. 5 (a) LMA with Front wheels on step edge; (b) LMA with flipper wheels at the rear

The coordinate of the COG on x_1 axis is given by:

$$G_{x1} = G_x \cos\theta - G_Y \sin\theta \qquad (2)$$

where θ is the robot's inclination, which is measured by the 3-axis compass. To avoid flipping over from the first step on the stairs, the COG must be maintained on the right side of y_1 axis. Therefore, the condition that $G_{x1} > 0$ must be satisfied. Substituting this condition into equation (2) and solving for G_x yields the following stability judgment equation:

$$G_x > G_y \tan\theta \qquad (3)$$

(ii) Stability Judgment Equation of LMA with Flipper at Rear

In the configuration shown in Fig. 5(b), LMA chassis has inclination θ, flipper angle φ (between 90 and 270^0), and the tip of the flipper sustains LMA on the ground. To avoid flipping over of the robot, the COG must be maintained at the right side of y' axis as indicated in Fig. 5(b). In order to fulfill this requirement, the condition that $G_{x1} > Q_{x1}$ must be satisfied. Solution of this condition for G_x yields the following stability judgment equation:

$$G_x > G_y \tan\theta + \frac{L}{2} + l(\varphi)\frac{\cos(\theta+\varphi)}{\cos\theta} \qquad (4)$$

(iii) Stability Judgment Equations of LMA on Nose Line

The required conditions for a mobile robot on a nose line have been researched [11]–[13]. These conditions are primarily: (i) half the wheelbase of a mobile robot is larger than the distance between two adjacent step edges; (ii) mobile robot's COG is over the step edge which the robot engages rearward. With these conditions the following equations were derived:

$$\theta \geq \sin^{-1}\frac{2h}{L/2 + l(180°) - r} \qquad (5)$$

$$G_x > \frac{L}{2} - l(180°) + \frac{h}{\sin\theta} + (G_y + r)\tan\theta \qquad (6)$$

B. Range of COG Coordinates

The position of the robot's COG is a function of the flipper angle. One of the methods to obtain the COG coordinate is to perform real-time calculations, which is undesirable as it significantly adds to the computation load. To avoid the realtime task, the range in which the LMA COG always stays was identified and used. In order to find the range, the relationship between the robot's COG position and its flipper angle was derived. With the derived equations we identified the maximum ($G_{x,\max}$) and minimum ($G_{x,\min}$) of the COG on the x coordinate (φ is 0 and 180^0, respectively) and the maximum ($G_{y,\max}$) and minimum ($G_{y,\min}$) of the COG on the y coordinate (φ is 90 and 270^0, respectively).

The COG of LMA always stays in the range defined by the four values above. Therefore, with those constant values, a real-time computation of COG position can be avoided and equations (3), (4), (5) and (6) are replaced by the following equations:

$$G_{x\min} > G_{y\max} \tan\theta \,, \tag{7}$$

$$G_{x\min} > G_{y\max} \tan\theta + \frac{L}{2} + l(\varphi)\frac{\cos(\theta+\varphi)}{\cos\theta} \,, \tag{8}$$

$$G_{x\min} > \frac{L}{2} - l(180°) + \frac{h}{\sin\theta} + (G_{y\max} + r)\tan\theta \tag{9}$$

C. Algorithms for Stability Judgments

During autonomous climbing of stairs, some tasks are simultaneously running, these includes: sending requests to the compass, receiving frames from the sensor and the remote controller and judging stability, and executing autonomous climbing procedures. In this section, the algorithms to stop LMA with stability equations are developed.

Derived stability judgment equation(s) corresponding to the robot's configuration are continuously evaluated based on up-to-date robot's inclination measurements, while the robot is moving. Once the issued equation(s) are violated, the robot shows a certain behavior, depending on the equation(s).

If equation (7) or (8) is not satisfied, LMA stops right away, and autonomous climbing terminates. This algorithm is named stability judgment thread 1 (abbreviated as S.J.T 1). The corresponding flowchart is shown in Fig. 6(a).

In the case that equation(s) (5) or/and (9) is violated, LMA stops right away and waits three seconds followed by another evaluation of both equations. Nevertheless, if both or either equation(s) is/are still not satisfied, autonomous climbing is terminated; otherwise, LMA restarts. The algorithm is called stability judgment thread 2 (abbreviated as S.J.T.2) and summarized in a flowchart shown in Fig. 6(b). This algorithm to stop LMA was incorporated to overcome the effects of noise associated with inclination data measurements while LMA is climbing stairs on a nose line. The effectiveness of the algorithms is validated, after an analysis of the noise in the inclination signal is discussed in Section V in the paper.

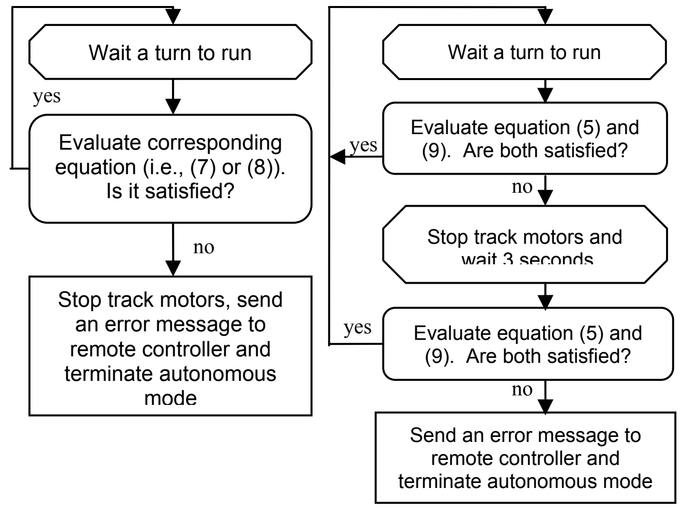

(a) (b)

Fig. 6 (a) Stability judgment thread 1; (b) Stability judgment thread 2

IV. Algorithms for Autonomous Climbing of Stairs

During autonomous climbing, LMA depends on measurements from its inclinometer (the 3-axis compass) and the encoders attached to the three motors. By interacting with those sensors, the algorithms to autonomously climb stairs are running based on climbing procedures mentioned earlier. The algorithms to autonomously climb stairs are divided into four stages: measuring step height, riding on the nose line, going on the nose line and landing. Furthermore, the stability judgments equations derived in Section 3 are incorporated in the algorithms as well. The algorithms mentioned above are executed in the following order: measuring step height, followed by, riding on nose line, then going on nose line, and ending with landing. In this section we focus on the algorithm developed for riding on the nose line.

Climbing Task Stage 3: Going on Nose line

In this stage, LMA moves forward on the nose line and continuously measures the slope of the nose line at the same time. The first motion of this stage is to move forward 50 cm, to assure that the flipper tip is detached from the ground. Then, LMA moves forward again while continuously measuring the inclinations. The velocity of forward motion is set to 3.2 cm/s and regulated by the closed-loop control of the drivers. During the motions, the stability judgment thread 2 as shown in Fig. 6(b) is continuously running. Since LMA is equipped with only the 3-axis compass and the encoders for the motors, it cannot detect the last step of the stairs. Therefore, it is expected that LMA is stopped by the operator when its front wheels are above the last step edge, at which time automatic landing stage is activated. Otherwise, LMA tracks will abruptly drop on the top step. In that case, LMA autonomously stops and autonomous climbing of stairs is completed. Although realized by the stability judgment, LMA halts the motion when its inclination shows a value less than 5^0. However, it is recommended and expected that the operator stops LMA to activate the automatic landing stage. The flowchart for going on nose line stage is shown in Fig. 7.

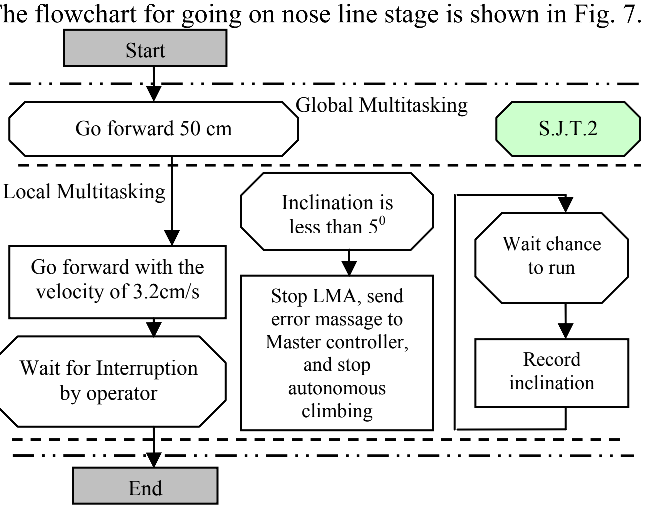

Fig. 7 Flowchart of going on nose line climbing stage

V. Experimental Setup and Results

The implementation and validation of autonomous climbing is detailed in this section. Several solutions to some problems occurred during the implementation stage are also discussed.

A. Signal Analysis and Filters

Autonomous climbing strongly relies on the pitch, or inclination data from the 3-axis compass embedded in the LMA chassis. The signal emanating from the compass had too excessive noise to be able to use it while it was moving on nose lines. Therefore, the signal was analyzed and algorithms and filters were designed in order to remove noise effects when the robot is moving on nose lines.

Signal Analysis

Fig. 8 shows raw inclinations signal from the 3-axis compass while LMA was moving on the nose line as shown in Fig. 9(c). When LMA is on the nose line, the inclination is supposed to provide readings indicating the slope of the nose line (i.e., 45^0). However, we observed that the signal is strongly disturbed by noise. After several observations of LMA motion, three main factors were found to cause the fluctuations in the signal emanating from the compass: (1) slips between the treads and step edges; (2) oscillation of the chassis; and (3) position of the LMA.

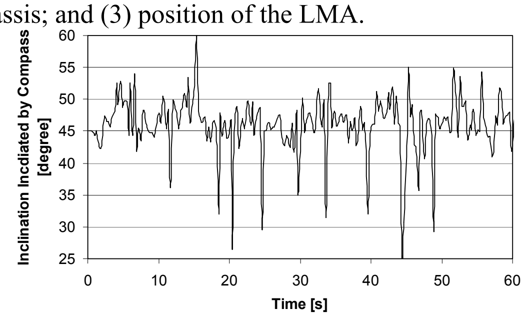

Fig. 8 Raw data from compass

Approximately 4 – 7 Hz noise is caused by LMA's frame the oscillations while it is moving on the nose line. This occurs when the tracks between the flipper wheels and the rear wheels locally bend when the stair edge touches the tracks in that area (Fig. 9(a)). Therefore, the compass shows a slightly larger value than the actual slope of the nose line. In cases when the step edges are positioned under the wheels as shown in Fig. 9(b), the inclination measured by the compass coincides with the actual slope of the nose line.

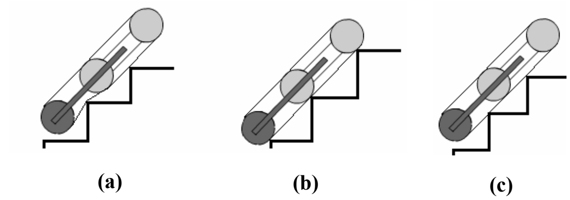

Fig. 9 Inclination changes with the position of the LMA

The deviations in the inclinations caused by LMA positions on the nose line were measured by a simple experiment under which LMA moves forward 1 cm, stops for five seconds, records the inclination data and repeats. By stopping for five seconds before the measurements are recorded, the noise caused by the tracks' slips and chassis oscillations are removed.

Noise Elimination

Two serially connected filters were designed in order to remove the noise from the measured inclination signal to guarantee stable autonomous climbing.

Filter 1: Algorithm for Pulse Elimination

With this filter, the abrupt pulses created by slip occurring between the treads and step edges were removed. In this algorithm, if the difference between new inclination data from the compass and the previous value is five degrees or more, the output of Filter 1 holds the same value; otherwise, the new value is outputted. This means that the data points from the compass are blocked until they settle within a certain range, thereby eliminating pulses having a magnitude of 5^0 or greater. Fig. 10 shows the simulated output of Filter 1 with its input being the raw data from the compass (Fig. 8). It can be seen that the pulses are being effectively truncated.

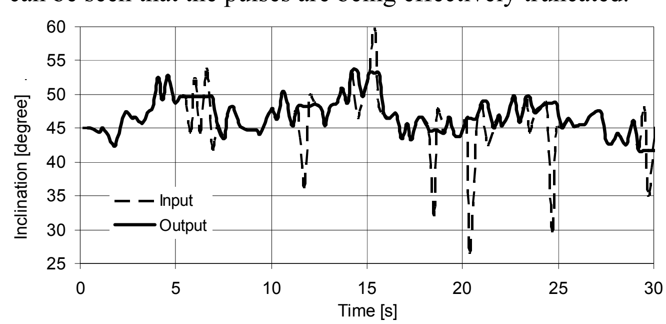

Fig. 10 Effects of Filter 1

Filter 2: Digital Filter

The second filter is a low-pass digital filter used to remove the noise caused by the oscillation of the chassis and other miscellaneous factors such as effects caused by electronic devices. The deviations created by LMA positions on a nose line are not considered noise, but rather real inclination changes that might cause LMA to flip over in some cases. Therefore, Filter 2 should pass those deviations. By considering their highest calculated frequency (0.137 Hz), the cut off frequency ($\mathbf{f_c}$) was set to 0.20 Hz. The frequency response of this filter confirmed that the filter is a LPF.

The two filters designed above were connected in series resulting in high frequency components being cut off after impulses are eliminated. With this set of filters, the raw data shown in Fig. 8 become the signal shown in Fig. 11. The output deviations from the slope of the nose line are restricted within seven degrees.

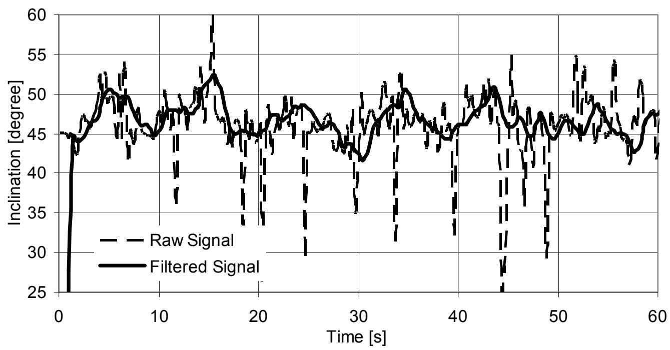

Fig. 11 Combined effect of Filters 1 and 2 connected in series

B. Validations & Results – Effectiveness of Noise Elimination

For the validation of Filters 1 and 2, new raw inclination signal and its filtered signal were directly read from LMA sensors. The signals from the LMA shown in Fig. 12 confirm that the pulses were successfully removed from the filtered signal around 66.5, 70.5, 79.5, 88, 90.5 and 95 seconds.

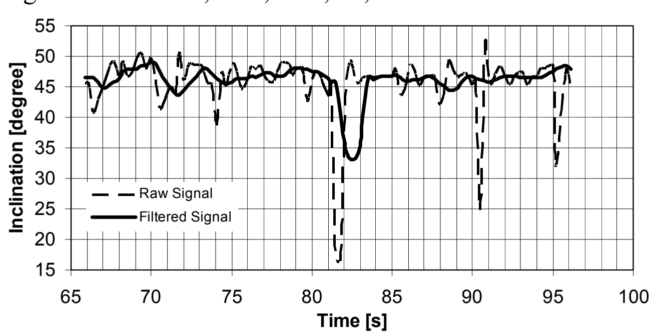

Fig. 12 Validation of noise elimination

Overall Validation

In order to examine the effectiveness of the entire motion sequences, LMA moved several times under autonomous climbing of stairs. In all cases, it was observed that autonomous climbing was successfully completed without any problems.

VI. Conclusions

The mechanical architecture of Linkage Mechanism Actuator (LMA) mobile robot was introduced, with a focus on procedures developed to climb stairs. Based on the procedures, algorithms under which LMA autonomously climbed stairs were developed. Stability judgment equations were also formulated and used as conditions to ensure tip-over stability of LMA depending on its configurations. The equations were incorporated into the stability judgments by which LMA autonomously stops. The theories and procedures used to obtain the data required for autonomous climbing were formulated and developed such as calculating LMA's COG using its COG range. The strong noise in the signals from the inclinometer was analyzed, and solutions to remove it with designed filters and algorithms were suggested and implemented. The solutions were validated, proving the successful implementation of autonomous climbing of stairs such that even untrained operators could have mobile robots climb stairs.

Acknowledgment

This work was partially supported by Natural Sciences and Engineering Research Council of Canada (NSERC), and Engineering Services Inc. (ESI).

References

[1] A.A. Goldenberg, J. Lin, "Variable Configuration Articulated Tracked Vehicle", US Patent Application # 11/196,486, August 4, 2005. Engineering Services Inc. http://www.esit.com

[2] J. Liu, Y. Wan, S. Ma, "Analysis of Stair-Climbing Ability for a Tracked Reconfigurable Modular Robot", Proc. of the 2005 IEEE Int. Workshop on Safety and Rescue Robotics, pp. 36-41, June 2005.

[3] J. Gaston, K. Raahemifar, and P.Hiscocks, "A Cooperative Network of Reconfigurable Stair-Climbing Robots," IEEE Int. Symp., May 2006.

[4] S.A. Stoeter and N. Papanikolopoulos, "Autonomous Stair-Climbing With Miniature Jumping Robots", Cybernetics, Vol. 35, No.2, 2005.

[5] X. Duan, Q. Huang, N. Rahman, J. Li and Jingtao Li, "MOBIT, A small Wheel–Track-Leg Mobile Robot," Proc. of the 6th Congress on Intelligent Control and Automation, Jun 21-23, 2006.

[6] D.G. Gweon and H.D. Kim, "Development of a mobile robot controlled by three motors for a hostile environment," Mechatronics Vol. 2, No. 1, pp. 43-64, 1992.

[7] W. Lee, S. Kang, M. Kim and K. Shin, "Rough Terrain Negotiable Mobile Platform with Passively Adaptive Double-Tracks and its Application to Rescue Missions," International Conference on Robotics and Automation, April 2005.

[8] B. Yamauchi, "PackBot: A versatile platform for military robotics", Proceedings of SPIE - Unmanned Ground Vehicle Technology VI, Vol. 5422, pp. 228-237, Orlando, FL, April 2004.

[9] Y. Xiong and L.Matthies, "Vision-Guided Autonomous Stair Climbing," Int. Conference on Robotics and Automation, April 2000.

[10] John D. Martens and Wyatt S. Newman, "Stabilization of a Mobile Robot Climbing Stairs," IEEE Int. Conf. on Robotics and Automation, Vol. 3, pp 2501-2507, 1994.

[11] J. Lin, "Studies on Movement Conditions of Tracked Vehicles with Variable Configuration," Eng. Services Inc., Oct., 2004, internal report.

[12] J. Lin, "Supplement 1- on "Movement Conditions of Tracked Vehicles", Engineering Serviced Inc., October 20, 2004, internal report.

[13] J. Lin, "Determining the Technology Parameters of LMA-2 Vehicle Based on Static Mechanics Analysis," Eng. Services Inc., May 2004, internal report.